Estimation of Regional Seasonal Variations in SERT-levels using the FreeSurfer PET pipeline: a reproducibility study

Martin Nørgaard[1*], Melanie Ganz[1,2], Claus Svarer[1,2], Vincent Beliveau[1,2], Patrick M. Fisher[1,2], Brenda Mc Mahon[1,2], Douglas N. Greve[3,4], Stephen C. Strother[5,6], and Gitte M. Knudsen[1,2]

[1] Neurobiology Research Unit, Copenhagen University Hospital, Rigshospitalet, DK-2100 Copenhagen, Denmark
[2] Center for Integrated Molecular Brain Imaging, Copenhagen University Hospital, Rigshospitalet, DK-2100 Copenhagen, Denmark
[3] Athinoula A. Martinos Center for Biomedical Imaging, Department of Radiology, Massachusetts General Hospital, Boston, MA, USA
[4] Harvard Medical School, Boston, MA, USA
[5] Rotman Research Institute at Baycrest, University of Toronto, Toronto, Canada
[6] Department of Medical Physics, University of Toronto, Toronto, Canada

Abstract. The purpose of this study was to assess the ability of the newly developed FreeSurfer (FS) PET processing pipeline to reproduce the results reported by Mc Mahon et al. 2014. Mc Mahon et al. 2014 investigated differences of the serotonin transporter (SERT) between summer and winter scans in patients suffering from Seasonal Affective Disorder (SAD) versus healthy controls, and for various genotypes. Seventeen SAD patients (8 men, 9 women; age, 27 ± 9 y) and 23 healthy controls (10 men, 13 women; age, 25 ± 7 y) underwent [^{11}C]-DASB PET imaging two consecutive times in a randomized sequence (winter or summer), defined by a 12 week interval centered around winter or summer solstice. A global volume weighted non-displacable binding potential (BP_{ND}) was estimated for all patients with the purpose of evaluating seasonal variation at the group level. We intended to evaluate reproducibility and consistency of the results reported by Mc Mahon et al. 2014 by comparing the corresponding results obtained with the newly developed FS PET pipeline, and with a special focus on current state-of-the-art methods. In general PET analysis using the FreeSurfer PET pipeline was able to reproduce the results estimated by gold standard procedures such as PVElab and SPM8. We were not able to obtain the exact same results as reported by McMahon et al., however this is likely to be caused by initial assumptions of volumes of interest and subsequent processing choices. The reported results seemed to be within an accepted range, indicating that FreeSurfer may be used as feasible tool in the analysis of PET data.

1 Introduction

Since the first published paper on Seasonal Affective Disorder (SAD) by Rosenthal and colleagues (1984), an increasing body of theoretical as well as exper-

imental hypotheses of the underlying pathology have accumulated and formed our modern notion of this phenomenon [1, 2]. It is estimated that up to 6% of the American population are affected by SAD, and additionally 15% may suffer from sub-syndromal SAD also referred to as "winter blues" [3]. In the human brain, SAD manifests itself as a mental condition characterized by a phasic occurrence of major depression during wintertime and with subsequent remission in summertime [1]. It is hypothesized to be in part triggered by a seasonal misregulation of the serotonin transporter (SERT), the mechanism by which endogenous serotonin (5-HT) is inactivated and recycled into the presynaptic terminal [2, 4]. These fluctuations are particularly evident in carriers of the short 5-HTTLPR polymorphism (S-allele carriers). In particular, healthy controls without any significant symptoms of seasonality show the ability to increase their cerebral SERT levels during summer as compared to winter, whereas SAD individuals show reduced cerebral SERT levels in the summer and increased levels in the winter [4]. The latter case effectively results in a decrease of endogenous serotonin, creating the typical symptoms related to SAD: reduced sex-drive, feelings of ineptitude, increased appetite, increased sleep and loss of energy [4].

State-of-the-art medical imaging techniques such as Positron Emission Tomography (PET) and Magnetic Resonance Imaging (MRI) can provide great insight into anatomical as well as functional properties of 5-HT transmission in the brain [5]. Ichise et al. [6] proposed a novel 2-parameter multilinear reference tissue model (MRTM2) using the highly selective radioligand [^{11}C]-DASB to model the complex kinetic properties of SERT. In addition, Kim et al. [7] reported a significant consistency in both reproduciblity and reliability of the MRTM2 in PET studies investigating SERT, as [^{11}C]-DASB correlates well with SERT density [8]. Recent developments in medical image processing allow the integration of even more sophisticated procedures such as cortical surface-based kinetic modeling of PET data. Greve et al. [9] utilized the newly developed FreeSurfer PET pipeline, and reported how surface-based analysis of PET data resulted in 2-4 times less intersubject variance resulting in 4 times fewer subjects needed in a group analysis to achieve the same statistical power. However, very little information regarding the effects of processing choices and reproducibility of PET data exists, and in order to validate new prospective processing pipelines further investigation is needed.

Therefore, in this paper we attempt to investigate the ability of the newly developed FreeSurfer PET processing pipeline to reproduce the results obtained from the current state-of-the-art processing pipeline reported by Mc Mahon et al. 2014 [4].

2 Methods

Subjects

Seventeen SAD S/L-allele carrying patients (8 men, 9 women; age, 27 ± 9 y) and 23 healthy S-allele carriers (10 men, 13 women; age, 25 ± 7 y) were enrolled

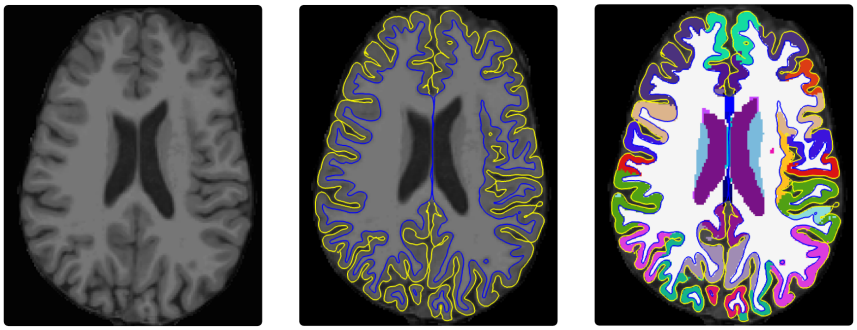

Fig. 1: **(a)** T1-weighted MP-RAGE sequence of the brain **(b)** FreeSurfer segmentation of the pial-surface (yellow) and white matter surface (blue) **(c)** FreeSurfer segmentation of cortical as well as subcortical regions.

from an ongoing longitudinal study investigating seasonal fluctuations in patients suffering from SAD versus healthy controls. All subjects were scanned biannually (winter and summer) in a randomized study-design, defined as a 12-week interval centered around winter or summer solstice. Recruitment and inclusion criteria were executed as described in [4].

PET Data Acquisition and Preprocessing

All patients were scanned using a Siemens ECAT High-Resolution Research Tomography (HRRT) scanner operating in 3D list-mode and with the highly selective radioligand [^{11}C]-DASB. The point spread function (PSF) inherent to the HRRT scanner was 4 mm. The imaging protocol consisted of a single-bed, 90 minutes transmission acquisition post injection of 590±21 (mean±SD) MBq, range 427-623 MBq, bolus into an elbow vein. PET data was reconstructed into 36 frames (6x10, 3x20, 6x30, 5x60, 5x120, 8x300, 3x600 seconds) using an iterative PSF reconstruction with attenuation map improvements (image matrix, 256 x 256 x 207; voxel size, 1.22 x 1.22 x 1.22 mm). The attenuation correction used in the reconstruction was based on a preliminary six minute TX transmission scan. Preprocessing of the PET data at the subject-level were in-scan motion corrected using AIR 5.2.5.
Prior to alignment, each frame was smoothed using a 10 mm Gaussian 3D kernel and thresholded at the 20-percentile level. Alignment parameters were estimated for PET frame 10-36 using AIR, geometrically transformed using a least squares cost-funtion, and resliced into a 4D motion corrected data set. This data set consisted of time activity curves (TACs) at each voxel and was used in the multimodal analysis described below [4]. An anatomical 3D T1-weighted MP-RAGE sequence with matrix size = 256 x 256 x 192; voxel size = 1 x 1 x 1 mm;

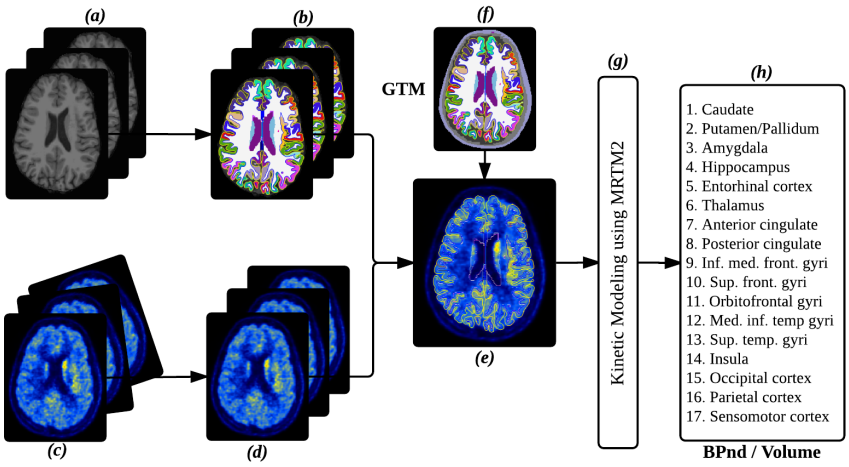

Fig. 2: **(a)** T1-weighted MP-RAGE conformed to 1 x 1 x 1 mm within FreeSurfer **(b)** FreeSurfer segmentation of the pial-surface (yellow), white matter surface (blue) and cortical as well as subcortical regions **(c)** Single-subject PET data aligned and motion-corrected using AIR 5.2.5 **(d)** PET TACs summed and averaged over all time-frames in order to estimate a weighted 3D image for co-registration **(e)** The averaged PET image aligned to the structural MRI using a boundary-based cost function with 6 degrees of freedom **(f)** Geometric transfer matrix (GTM) created within FreeSurfer (segmenting CSF, skull, air cavities, and the rest of the head) **(g)** Kinetic modeling of GTM TACs using MRTM2 **(h)** Estimation of regional BP_{ND} and corresponding volumes for 17 different brain regions.

TR/TE/TI = 1550/3.04/800 ms; flip angle = 9° was additionally acquired for all subjects using a Siemens Magnetom Trio 3T MR scanner or a Siemens 3T Verio MR scanner. This image was co-registered to the average PET image. All single-subject MRI sequences were prior to further analysis non-linearly gradient corrected for spatial distortions according to Jovicich et al. [10]. The distortion correction was performed to correct for MR gradient nonlinearities in order to achieve optimal PET-MR co-registration.

Processing in FreeSurfer

All MR scans were processed and analyzed using FreeSurfer [11] (http://surfer.nmr.mgh.harvard.edu, version 5.3) and MATLAB R2013a (8.1.0.604) 64bit. FreeSurfer contains a fully automatic pipeline for processing of cross-sectional as well as longitudinal structural imaging data. Furthermore, it includes several features such as skull stripping, B1 bias field correction, non-linear registration to a stereotaxic atlas, statistical analysis of morphometric differences, and labeling of

cortical/subcortical brain structures (Figure 1) [11]. As described previously, all single-subject PET TACs were initially estimated as a time-weighted sum over all time-frames in order to estimate a weighted 3D image for co-registration. Subsequently, the mean PET image was aligned to the structural MRI using a rigid intra-subject multimodal registration utilizing a boundary-based cost function with 6 degrees of freedom [12]. Within the FreeSurfer PET framework an additional segmentation matrix was created by segmenting CSF, approximate skull, air cavities, and the rest of the head. The segmentation was utilized within the geometric transfer matrix framework (GTM), assuming all VOIs have a constant but unknown TAC [9, 13]. More specifically, we were able to extract a single TAC from each respective VOI and subsequently perform kinetic modeling (KM) using MRTM2 with high-binding regions caudate, putamen, pallidum and thalamus, and the cerebellum as reference region (Figure 2) [6]. The final outcome from FreeSurfer was a set of 17 regional non-displaceable binding potentials (BP_{ND}). In comparison, Mc Mahon et al. [4] used SPM8 to segment and co-register the high-resolution MR and PET images. Independent automatic delineation of VOIs was performed within the PVElab framework using probability maps based on ten high-resolution MR templates [15]. Templates were transferred from template to subject space using a 12-parameter registration followed by a fully flexible voxel based warping [16], and the probability of a given voxel belonging to a specific VOI was determined as the average of all transferred VOI templates [4].

Statistical Analysis

Data are expressed as mean±SD. Normality plots were used to verify the normality assumptions of the data and to eliminate possible outliers. To test for structural differences between summer and winter scans, we estimated the volumes of the regions in the GTM segmentation in FreeSurfer and evaluated the paired difference. A global BP_{ND} (gBP_{ND}) was estimated as a volume-weighted average of whole brain [^{11}C]-DASB BP_{ND} as in Mc Mahon et al. [4] based on the seventeen gray matter segmented brain regions (v_i) listed in Figure 2.

$$gBP_{ND} = \frac{\sum_{i=1}^{17} BP_{ND,i} \times v_i}{\sum_{i=1}^{17} v_i} \tag{1}$$

The exact corresponding brain regions were not available in FreeSurfer, however a visual approximation of the similar brain regions were obtained in agreement with an experienced neuroscientist. Global BP_{ND} was estimated for all 17 brain regions to investigate the variation in the two processing streams.

3 Results

Structural Evaluation

Mean volume of the 17 regions separated into the SAD and HC groups was calculated for all patients, and summarized as mean±SD for both consecutive scans

(summer and winter). All mean volume characteristics are visualized in Figure 3, where significant volume variations between the two streams were observed for both subcortical and cortical regions. Differences in structural volume between summer and winter scans were tested for statistical significant difference using a paired t-test. The t-test failed to reject the null hypothesis for all 17 regions of interest (Bonferroni corrected), indicating no significant structural changes with respect to summer and winter scans (Figure 3). Nonetheless, we observed

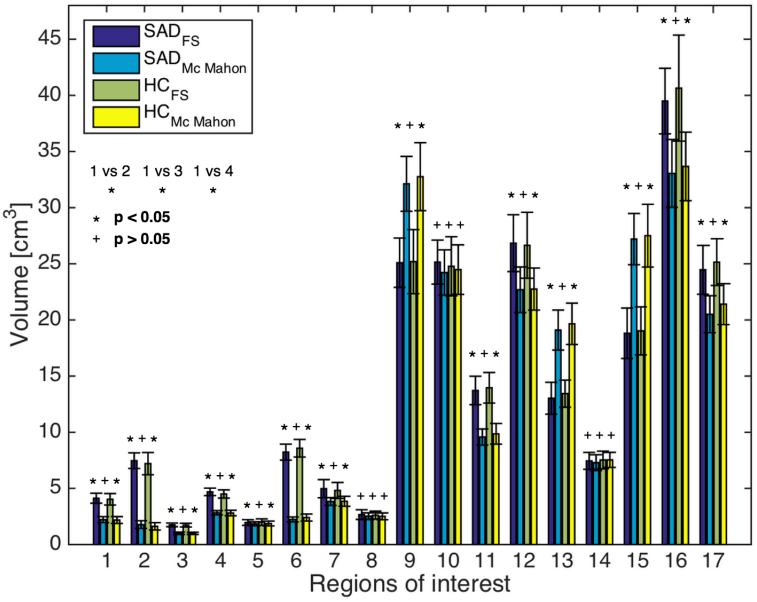

Fig. 3: Seasonal mean volume for all regions of interest (n = 17 SAD, n = 23 HC); two processing streams and two subgroups. The errorbars indicate the subject variation. + indicates p>0.05 and * indicates p<0.05 for the 3 tests; 1 vs 2, 1 vs 3 and 1 vs 4.

a significant volume difference in 14 of the total 17 regions comparing the processing results from Mc Mahon et al. [4] and FreeSurfer (Bonferroni corrected). The significant regions were 1 (caudate), 2 (putamen/pallidum), 3 (amygdala), 4 (hippocampus), 5 (entorhinal cortex), 6 (thalamus), 7 (anterior cingulate), 9 (inferior medial frontal gyri), 11 (orbitofrontal cortex), 12 (medial inferior temporal gyri), 13 (superior temporal gyri), 15 (occipital cortex), 16 (parietal cortex) and 17 (sensomotor cortex). Only for three of the fourteen significantly different regions, namely region 9 (inferior medial frontal gyri), region 13 (superior temporal gyri) and region 15 (occipital cortex), was the FreeSurfer volume lower than reported by Mc Mahon et al. [4], whereas for the remaining regions the opposite effect was observed. Furthermore, we observed a similar relative difference in volume between the two subgroups in each respective processing stream.

This effect indicates that the difference in volume between the two processing streams is most likely to be driven by the choice of VOIs.

Reproducibility of Regional BP_{ND}

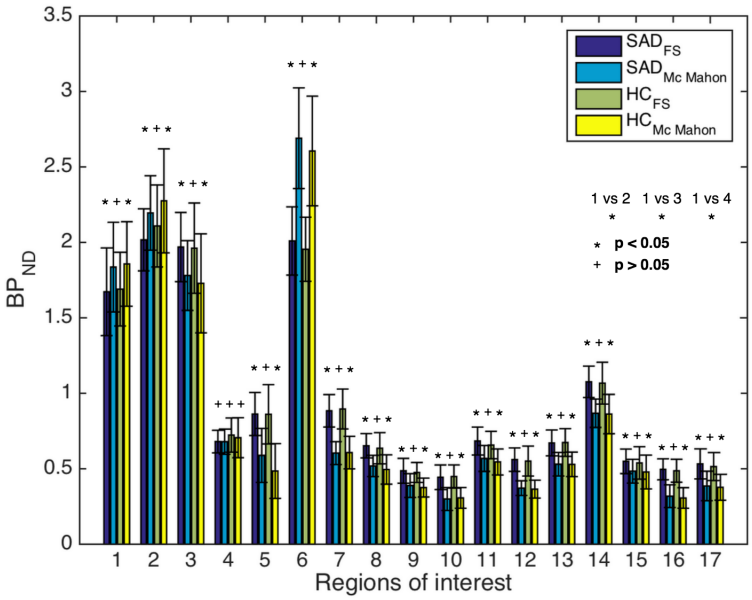

Fig. 4: Seasonal mean BP_{ND} values for all regions of interest (n = 17 SAD, n = 23 HC); two processing streams and two subgroups. The errorbars indicate the subject variation. + indicates p>0.05 and * indicates p<0.05 for the 3 tests; 1 vs 2, 1 vs 3 and 1 vs 4.

We also investigated the variation of the BP_{ND} as exemplified in Figure 4. Overall, the aim was to evaluate if the binding potential was dependent on the choice of VOI as well as the processing pipeline. We estimated the regional BP_{ND} for all subjects and for both consecutive scans (80 scans). Differences in BP_{ND} between summer and winter scans were tested for statistical significant difference using a paired t-test. The t-test failed to reject the null hypothesis for all 17 regions of interest (Bonferroni corrected), indicating no significant BP_{ND} changes with respect to summer and winter scans.
Consequently, for each respective region we therefore pooled the summer BP_{ND} and winter BP_{ND} into a single-subject mean value (Figure 4). Significant regional BP_{ND} differences between the two processing streams were tested using a two-sided t-test. The t-test failed to reject the null-hypothesis for only 1 of the 17 regions, namely the hippocampus ($p = 0.69$), Bonferroni corrected. Subsequently, we tested for regional BP_{ND} differences within the groups HC and

SAD for both processing streams using a two-sided t-test, in order to determine seasonal BP_{ND} changes. The t-test failed to reject the null-hypothesis for all regions, indicating no significant BP_{ND} differences between HC and SAD, and within each respective processing stream. The results of the two tests are summarized in Figure 4.

Reproducibility of Global BP_{ND}

Consequently, since the difference in regional BP_{ND} revealed significantly different results in terms of processing choice, we intended to investigate how the volume and BP_{ND} differences using the FreeSurfer stream would affect the global BP_{ND}. The global BP_{ND} was estimated for all subjects and for both scans. In Table 1 the mean global BP_{ND} ± SD is visualized for 4 subgroups of the data, namely; HC, SAD, SAD s-carriers only and SAD L_A/L_A only. The global BP_{ND} was estimated for all 4 subcategories, both in winter and summer. The only significant global variation was observed for HC subjects ($p = 0.01$). This result was also reported by Mc Mahon et al. [4], however, large variations in p-values was additionally observed between the two processing pipelines for SAD all genotypes and SAD L_A/L_A, respectively.

HC	Summer	Winter	P-value
FreeSurfer	0.7 ± 0.09	0.66 ± 0.06	**0.01***
Mc Mahon	0.49 ± 0.08	0.46 ± 0.06	**0.01***
SAD, all genotypes	Summer	Winter	P-value
FreeSurfer	0.68 ± 0.07	0.69 ± 0.07	0.49
Mc Mahon	0.47 ± 0.07	0.50 ± 0.06	0.10
SAD, s-carriers only	Summer	Winter	P-value
FreeSurfer	0.67 ± 0.07	0.7 ± 0.06	0.10
Mc Mahon	0.45 ± 0.07	0.51 ± 0.05	0.18
SAD, L_A/L_A only	Summer	Winter	P-value
FreeSurfer	0.71 ± 0.07	0.68 ± 0.09	0.16
Mc Mahon	0.49 ± 0.06	0.48 ± 0.07	0.50

Table 1: Seasonal global BP_{ND} changes, subjects categorized into four subgroups, namely; HC, SAD, SAD s-carriers only and SAD L_A/L_A only. Values reported in [4] have changed due to a processing error, and we are here presenting the correctly updated values.

4 Discussion

The present study examined symptomatic/asymptomatic variations in SAD versus healthy controls using PET analysis in FreeSurfer. The study by Mc Mahon

et al. [4], from which this data was derived from, is the first to investigate SERT binding differences in a longitudinal study design for both SAD subjects and healthy controls. The VOIs between the two processing pipelines showed large volume variations for both cortical and subcortical regions. More specifically, the respective VOIs were consistenly larger in FreeSurfer compared to Mc Mahon et al. [4] where large variations were observed in particular for the subcortical regions. Region 1 (caudate), 2 (putamen/pallidum) and 6 (thalamus) volumes in FreeSurfer yielded a 184%, 433% and 361% increase in volume size, respectively, compared to the SPM8 segmented volumes reported by Mc Mahon et al. [4]. This is mainly influenced by the segmentation of the T1-weighted image in SPM8, which segments the T1 into gray matter (GM), white matter (WM) and cerebrospinal fluid (CSF) using three different probability maps. The division of subcortical structures into subgroups highly affects the comparison of the two processing pipelines, as FreeSurfer omits the segmentation of subcortical structures into GM and WM. The effect is visualized in Figure 5, highlighting the significant volume differences for region 2 (putamen+pallidum) and region 6 (thalamus) using SPM8 and FreeSurfer. FreeSurfer contains an automatic individualized segmentation pipeline for dividing cortical and subcortical structures. In particular, FreeSurfer performs an excellent job in segmenting cortical GM, and it is therefore reasonable to assume that the differences in volume between FreeSurfer and SPM8 are not biased by the GM/WM segmentation as observed for the subcortical regions. The corresponding VOIs chosen by Mc Mahon et al. [4] were visually selected in agreement with an experienced neuroscientist. Therefore it was also expected that an exact compliance in choice of volume for the two pipelines was not possible.

The regional BP_{ND} values between the two studies were also evaluated. The MRTM2 in FreeSurfer showed comparable BP_{ND} values for the respective VOIs in relation to Mc Mahon et al. [4]. The BP_{ND} variability between the two streams ranged from 46% to 75%, with the largest variation observed in the cortical regions and with the highest BP_{ND} values observed using FreeSurfer. Only the BP_{ND} values for region 1 (caudate), 2 (putamen+pallidum) and 6 (thalamus) were higher in Mc Mahon et al. compared to FreeSurfer. This effect may be explained by the significant regional difference between FreeSurfer and SPM8, where a more specific choice of region size would exclude possible voxels containing low BP_{ND}, thereby resulting in a regional increase of the average BP_{ND}. Furthermore, the high-binding TAC will most likely be different from one stream to another, as the subcortical regions are used for extracting the high-binding TAC. This would in turn result in a different estimate of k_2', and possibly a bias in the KM. In addition, an increase in region size using FreeSurfer may increase the probability of including low BP_{ND} areas, thereby significantly contributing to a decrease in regional BP_{ND}. However, the division of subcortical structures into GM and WM in SPM8 is in fact a critical omission with respect to [^{11}C]-DASB PET imaging, as the BP_{ND} values within these regions seem to be uniformly distributed (Figure 6). The effect of higher BP_{ND} values reported by Mc Mahon et al. [4] was only observed for the subcortical regions 1, 2 and 6,

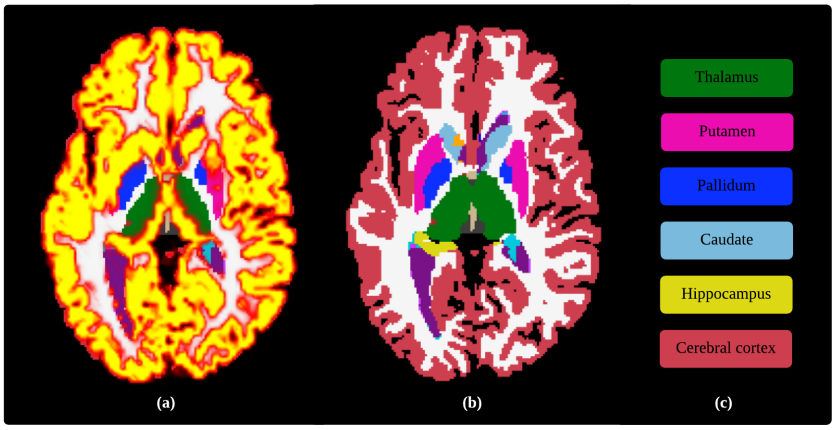

Fig. 5: **(a)** Segmented gray matter regions in SPM (shown in yellow-red) superimposed to the segmentation performed by FreeSurfer **(b)** Segmentation of subcortical regions in FreeSurfer **(c)** Regions of interest with specified color-labeling according to the segmentation in (b).

indicating that FreeSurfer may perform better in segmenting cortical structures compared to PVElab and SPM8, as both an increase in volume and BP_{ND} were observed for these regions.

In this study we were especially interested in investigating the effects of the FreeSurfer PET stream in order to reproduce the results reported by Mc Mahon et al. [4]. Mc Mahon and colleagues [4] estimated a single-subject volume weighted average of whole brain [^{11}C]-DASB BP_{ND} (global BP_{ND}) based on seventeen volume weighted gray matter segmented regions. The global BP_{ND} was consistently larger in all cases using the FreeSurfer pipeline compared to Mc Mahon et al. [4]. This increase seems to be in consistency with the definition of the weighted global BP_{ND}, where an increase in BP_{ND} values and an increase in volume sizes results in an increase of global BP_{ND}. Nevertheless, we did not find any significant relative differences in BP_{ND} nor in volume sizes using the results reported by either FreeSurfer or Mc Mahon et al. [4]. However, the fact that both SAD s-carriers only and SAD L_A/L_A carriers only reveal tendencies of statistical significance using the FS pipeline, may indicate that these subgroups regulate their SERT levels differently, as the tendency is eliminated for SAD all genotypes. Mc Mahon et al. [4] investigated whole brain SERT (global BP_{ND}) as primary outcome measure, arguing that BP_{ND} values are highly correlated across brain regions and that seasonal changes have been described in various brain regions [4]. However, a global measure capturing all brain regions and BP_{ND} into a single estimate may exclude important diagnostic information that are present in the data. The FreeSurfer PET pipeline faciliates a solution to this lack of information by offering a surface-based PET analysis, where cortical smoothing results in 2-

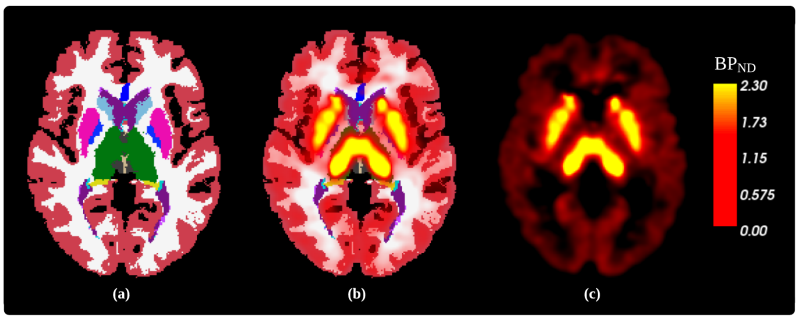

Fig. 6: **(a)** Segmentation of subcortical regions in FreeSurfer **(b)** Segmentation of subcortical regions in FreeSurfer superimposed with a corresponding BP_{ND} map **(c)** BP_{ND} map filtered with a 5 mm Gaussian 3D kernel showing high radioligand uptake in the regions thalamus, caudate, putamen and pallidum.

4 times reduced intersubject variance. Next step would be an analysis of the same cohort, SAD and HC in a univariate/multivariate framework, which may support a regional seasonal effect related to SERT. Furthermore, it is of great interest to contain both the processing and modeling within the same framework as provided in FreeSurfer, whereas the processing by Mc Mahon et al. [4] used different pipelines for each processing step to approach the final results. This may lower the probability of making a user-dependent mistake, which is highly critical in an inter-subject analysis.

5 Conclusion

In conclusion, PET analysis using the FreeSurfer PET pipeline is able to reproduce the results estimated by gold standard procedures such as PVElab and SPM8. We were not able to reproduce the exact same results reported by McMahon et al. [4] investigating the global BP_{ND}, however this may in part be driven by initial assumptions of the VOIs. Nevertheless, the reported results seemed to be distributed within an accepted range. Future perspectives may include voxelwise studies, where healthy controls and SAD patients are tested in a univariate/multivariate framework.

References

[1] NE Rosenthal, DA Sack, JC Gillin, AJ Lewy, FK Goodwin, Y Davenport, PS Mueller, DA Newsome, and TA Wehr. 1984. Seasonal Affective Disorder. A Description of the Syndrome and Preliminary Findings with Light Therapy. Archives of General Psychiatry 41(1): 72–80.

[2] J Kalbitzer, D Erritzoe, KK Holst, FA Nielsen, L Marner, S Lehel, T Arentzen, et al. 2010. Seasonal Changes in Brain Serotonin Transporter Binding in Short Serotonin Transporter Linked Polymorphic Region-Allele Carriers but Not in Long-Allele Homozygotes. Biological Psychiatry 67(11): 1033–39.

[3] DH Avery, D Kizer, MA Bolte, and C Hellekson. 2001. Bright Light Therapy of Subsyndromal Seasonal Affective Disorder in the Workplace: Morning vs. Afternoon Exposure. Acta Psychiatrica Scandinavica 103 (4): 267–74.

[4] B Mc Mahon, SB Andersen, MK Madsen, LV Hjordt, I Hageman, H Dam, C Svarer, S da Cunha-Bang, W Baare, J Madsen, L Hasholt, K Holst, VG Frøkjær, GM Knudsen. 2014. Seasonal difference in brain serotonin transporter binding predicts symptom severity in patients with seasonal affective disorder. http://www.ecnp-congress.eu/presentationpdfs/7/P.1.i.037.pdf.

[5] NM Barnes, and T Sharp. 1999. A Review of Central 5–HT Receptors and Their Function. Neuropharmacology 38(8): 1083–1152.

[6] M Ichise, JS Liow, JQ Lu, A Takano, K Model, H Toyama, T Suhara, K Suzuki, RB Innis, and RE Carson. 2003. Linearized Reference Tissue Parametric Imaging Methods: Application to [11C]DASB Positron Emission Tomography Studies of the Serotonin Transporter in Human Brain. Journal of Cerebral Blood Flow and Metabolism 23(9): 1096–1112.

[7] JS Kim, M. Ichise, J Sangare, and RB Innis. 2006. PET Imaging of Serotonin Transporters with [C-11]DASB: Test-Retest Reproducibility Using a Multilinear Reference Tissue Parametric Imaging Method. Journal of Nuclear Medicine 47(2): 208–14.

[8] N Ginovart, AA Wilson, JH Meyer, D Hussey, S Houle. Positron emission tomography quantification of [11C]-DASB binding to the human serotonin transporter: modeling strategies. J Cereb Blood Flow Metab. 2001;21: 1342–1353.

[9] DN Greve, C Svarer, PM Fisher, L Feng, AE Hansen, W Baare, B Rosen, B Fischl, and GM Knudsen. 2014. Cortical Surface–Based Analysis Reduces Bias and Variance in Kinetic Modeling of Brain PET Data. Neuroimage 92: 225–36.

[10] J Jovicich, S Czanner, DN Greve, E Haley, A van der Kouwe, R Gollub, D Kennedy, et al. 2006. Reliability in Multi–Site Structural MRI Studies: Effects of Gradient Non–Linearity Correction on Phantom and Human Data. Neuroimage 30(2): 436–43.

[11] B Fischl. 2012. FreeSurfer. Neuroimage 62 (2): 774–81.

[12] DN Greve, and B Fischl. 2009. Accurate and Robust Brain Image Alignment Using Boundary-Based Registration. NEUROIMAGE 48(1): 63–72.

[13] OG Rousset, Y Ma, and AC Evans. 1998. Correction for Partial Volume Effects in PET: Principle and Validation. Journal of Nuclear Medicine, J. Nucl. Med 39(5): 904–11.

[14] C Destrieux, B Fischl, A Dale, and E Halgren. 2010. Automatic Parcellation of Human Cortical Gyri and Sulci Using Standard Anatomical Nomenclature. Neuroimage 53(1): 1–15.

[15] C Svarer, K Madsen, SG Hasselbalch, LH Pinborg, S Haugbol, VG Frokjr, S Holm, OB Paulson, and GM Knudsen. 2005. MR-Based Automatic Delineation of Volumes of Interest in Human Brain PET Images Using Probability Maps. Neuroimage 24 (4): 969–79.

[16] U Kjems, SC Strother, J Anderson, I Law, and LK Hansen. 1999. Enhancing the Multivariate Signal of [O-15] Water PET Studies with a New Nonlinear Neuroanatomical Registration Algorithm. IEEE TMI 18(4): 306–19.